# Simultaneous inversion of velocity and reflectivity

Yang Yang[1*], Jaime Ramos-Martinez[1], Dan Whitmore[1], Guanghui Huang[1] and Nizar Chemingui[1]
describe a new seismic inversion workflow to simultaneously invert for velocity and reflectivity.

## Abstract

We describe a new seismic inversion workflow to simultaneously invert for velocity and reflectivity. With a single modelling engine, parameterized in terms of velocity and vector reflectivity, the two earth properties are iteratively updated using their appropriate sensitivity kernels based on inverse scattering theory. The vector reflectivity is estimated as a data domain least-squares migration and is the key for updating the velocity model beyond the maximum penetration depth of refracted and diving wave energy. With field examples, we demonstrate how the new solution for vector-reflectivity modelling combined with proper inversion kernels enable us to address the long-standing challenge of building full-bandwidth earth models.

## Introduction

The main goal of seismic inversion is to obtain a detailed estimation of subsurface properties, primarily velocity and reflectivity. The classical inversion workflow consists of two sequential steps based on scale separation of the earth model, i.e., building the long wavelength velocity model, and imaging the reflectors associated with geological boundaries. Over the past decade, FWI has emerged as an optimal solution for velocity estimation. It utilizes optimization methods to recover an earth model which generates modelled data that best matches the recorded seismic data. The inversion process maps the data misfit (difference between modelled and recorded data) to velocity perturbations in the subsurface. In principle, FWI is capable of recovering a complete earth model with a resolution dictated by the seismic experiment. In practice, and more than three decades after its conception (Tarantola, 1984), FWI is still evolving to deliver on that promise. The problem is not the theory itself, but most often negligence to recognize seismic inversion as a two-goal process. The earth model can be represented as a smoothly varying (low-wavenumber) velocity macro-model onto which are superimposed sharp contrasts in acoustic properties (high-wavenumbers) associated with geological boundaries and expressed as reflectivity (e.g., Mora, 1989). The goal of seismic inversion is to both estimate the velocity and predict the reflectivity without damaging either.

In recent years, Least-Squares Reverse Time Migration (LS-RTM) has become the method of choice for seismic reflectivity inversion in complex geological settings. In theory, the data domain LS-RTM algorithm is similar to FWI, which also aims at minimizing the differences between the modelled and recorded data. Accordingly, it is natural to solve both problems in a joint scheme where each inversion targets a specific scale representation of the earth model.

Conventional FWI estimates of the velocity mainly rely on refracted and diving waves. By using sufficient long offset data and properly handling the cycle-skipping problem, FWI can recover a good velocity model up to the maximum penetration depth of diving waves. Consequently, the need to recover velocities at deep targets has triggered demand for long offset acquisitions. As an alternative, one can utilize reflections to recover velocities beyond the penetration depth of refracted energy (e.g., Xu et al., 2012; Zhou et al., 2015). However, in order to use reflections in FWI, scale separation of the inversion gradient is essential for minimizing the crosstalk between velocity and impedance during the inversion. Moreover, combining both low- and high-wavenumber components in FWI slows down the convergence of the inversion and increases the risk of being trapped into local minima.

We present a novel seismic inversion approach to simultaneously invert for velocity (FWI) and reflectivity models (LS-RTM). The joint inversion has been previously applied in a nested fashion (e.g., Zhou et al., 2015; Chi et al., 2017), but the cost increase is significant. Berkhout (2012) proposed a joint migration inversion solution using a modelling engine that relies on waves propagating in the up/down directions. Consequently, the estimation of the velocity does not consider refracted and diving waves (Verschuur et al., 2016). In our solution, we use a wave-equation modelling relation that is parameterized in terms of velocity and vector reflectivity and capable of modelling the full seismic wavefield. A key aspect of the inversion is the separation of the low- and high-wavenumber components of the gradient, enabling the sensitivity kernels to update the velocity and the vector reflectivity, respectively (Whitmore and Crawley, 2012; Ramos-Martinez et al., 2016). With minimal pre-processing of the input data, the output of the inversion is a velocity model that fits the kinematics of all recorded events, and a good estimate of the earth's reflectivity compensated for acquisition and poor illumination effects.

We first describe the theory supporting the new simultaneous inversion, then we show its performance using a controlled

[1] PGS
[*] Corresponding author, E-mail: Yang.Yang@pgs.com
DOI: 10.3997/1365-2397.fb2021091

experiment and two field surveys from the Gulf of Mexico and the Campos Basin in Brazil.

## Simultaneous velocity and reflectivity inversion

FWI and LS-RTM share a similar framework, both aiming at the minimization of the misfit between modelled and recorded data. Accordingly, it's possible to solve both problems in a joint scheme. The most common approach is to augment the wave equation with an additional Born modelling relation (Mora, 1989) that is based on a first-order approximation to perturbation theory. In our workflow, we use the acoustic wave equation parameterized in terms of velocity and vector reflectivity (Whitmore et al., 2020) by reformulating the variable density acoustic wave equation. With no approximation in this reformulation, our modelling relation is capable of generating the full acoustic wavefield, including refracted and reflected energy as well as free-surface and internal multiples.

The velocity and the vector reflectivity are computed based on their appropriate kernels after scale separation and the inversion updates of both parameters during each iteration. The simultaneous inversion workflow is summarized in Figure 1. A starting velocity model is required for the inversion while an initial reflectivity is computed during the first iteration as an RTM image.

## Overthrust synthetic example

A modified version of the SEG/EAGE overthrust model is used to demonstrate the benefits of the simultaneous inversion. We simulate the input data by solving the variable density wave-equation using the true velocity and density models (Figures 2a and 2b). The true reflectivity (e.g., vertical reflectivity) is shown in Figure 2d. We use a heavily smoothed velocity field as a starting model. The maximum frequency in the data is about 25 Hz while the maximum offset is 4 km. Therefore, the inversion is mostly driven by reflections. Figures 1e and 1f show the results of the simultaneous inversion. The inverted velocity correctly retrieves the detailed features in the velocity model. Similarly, the inverted reflectivity is equivalent to the true one. While all components of the vector reflectivity are used in the inversion, only the vertical component is displayed in Figure 2.

## Field data examples

The performance of the new simultaneous inversion is illustrated using two field datasets. In both examples, we start from simple initial velocity models and zero reflectivity. We use the total pressure data with minimal data pre-processing that included receiver-motion correction and noise attenuation.

The first example is from the deep-water Gulf of Mexico, De Soto Canyon area. The data were acquired with multisensor streamers and with a maximum offset of 12 km. No particular mutes or events were selected; therefore, all recorded data were used for the inversion. Figure 3a shows the initial velocity model while Figure 3c displays the reflectivity from the first iteration of the inversion, which is equivalent to an RTM image

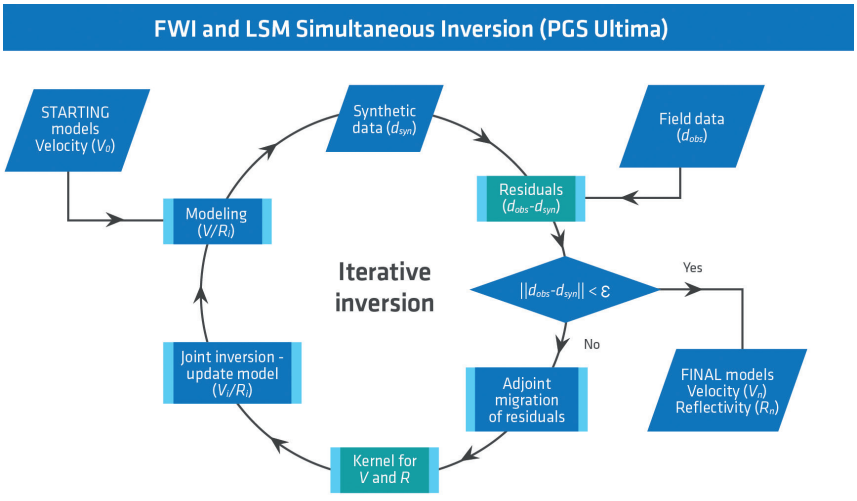


**Figure 1** A schematic of the full wavefield velocity and reflectivity simultaneous inversion approach.

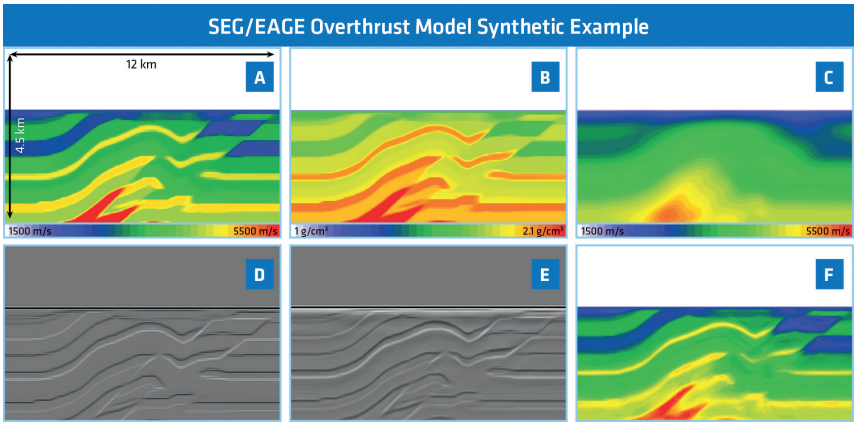


**Figure 2** Overthrust model synthetic test example. True velocity (a) and density (b) models. (c) Initial velocity model. (d) True vertical reflectivity. (e) Inverted vertical reflectivity and (f) velocity from the simultaneous inversion.

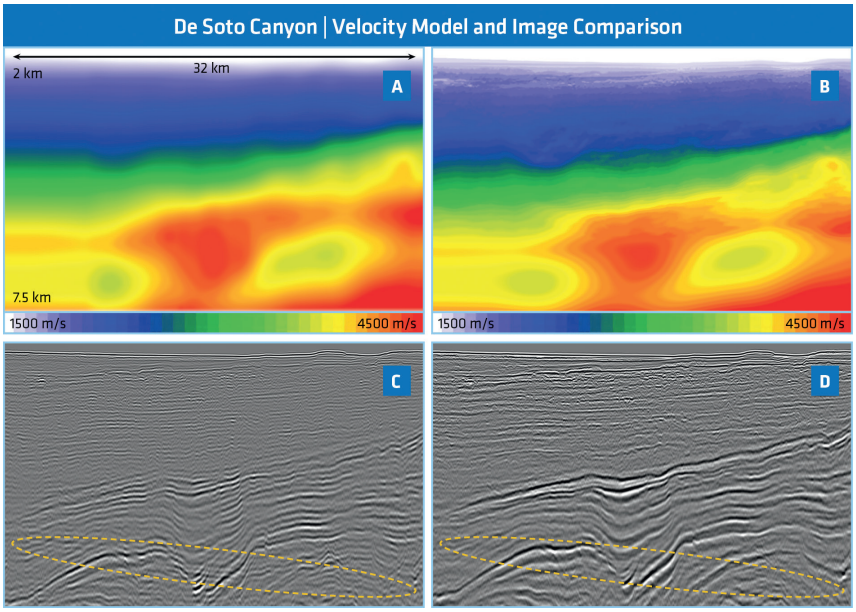


**Figure 3** De Soto Canyon field data example. (a) Initial and (b) inverted velocity models. (c) Vertical reflectivity from first iteration. (d) Final inverted vertical reflectivity. Notice the crosstalk reduction as the yellow oval indicates.

using the starting velocity model. Since the data contained multiples, crosstalk artifacts are observed in the RTM image and are indicated by the yellow oval. The results after several iterations of simultaneous inversion are shown in Figures 3b and 3d. The inverted models clearly display higher resolution. Also notice the reduction of the crosstalk in the final reflectivity model.

The second field data example is from a deepwater environment in the Campos Basin, offshore Brazil. Although the maximum inline offset in the survey is 10 km, the water column of more than 3 km makes it challenging to update the deep targets using refracted energy. We applied the simultaneous inversion to the total pressure data using full shot records (i.e., no event selection). Figures 4a and 4b show the vertical reflectivity models corresponding to the first and final iteration of the inversion while the velocity updates are displayed in Figure 4c, superimposed on the final reflectivity. The velocity updates extend beyond the maximum penetration depth of the diving waves. Note the improvement in the resolution of the shallow fault system (orange and blue ovals). Moreover, there is a coherency enhancement in the deep reflectors in the mini-basin and the steep salt flanks (orange and blue arrows). Validation of the results is supported by the image gathers computed from the initial and the final velocity models and shown in Figures 5a and 5b. Similarly, a depth slice at 3.4 km from the initial velocity model (Figure 6a) is compared with the final FWI model (Figure 6b) showing clear enhancement in the spatial resolution conformable to the structure.

Figure 7 shows another inline section that illustrates the velocity updates in the complex model, including the salt. Also, shown in Figure 7c, is the horizontal reflectivity image where energy is observed mainly around the steep salt flanks.

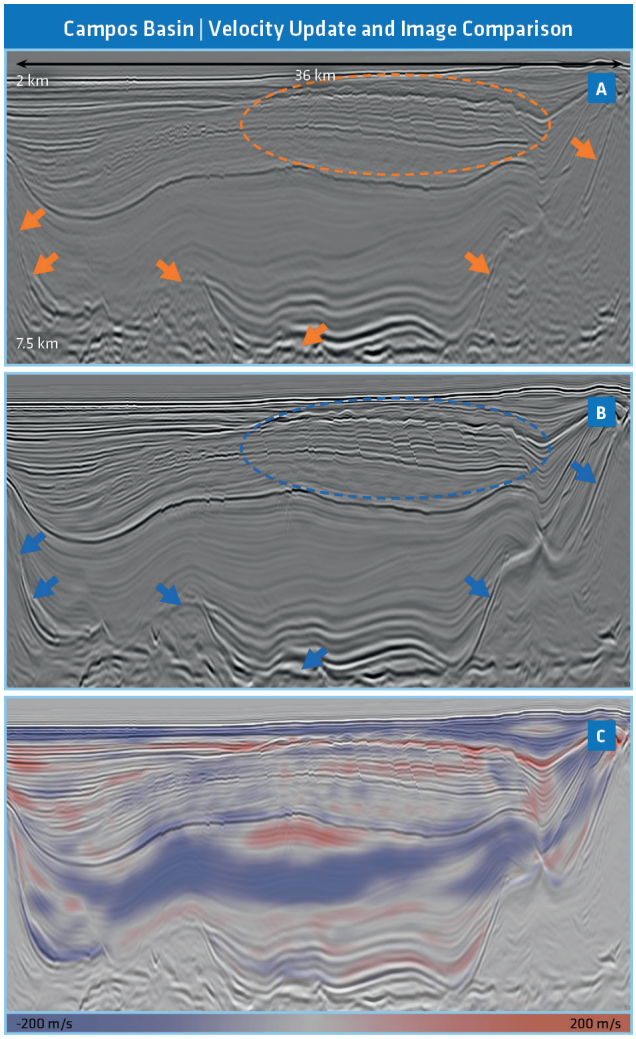


**Figure 4** Campos Basin field data example. (a) Vertical reflectivity from first iteration. (b) Final inverted vertical reflectivity. (c) Velocity updates on final vertical reflectivity.

## Conclusions

We introduced a non-linear iterative inversion solution to simultaneously estimate velocity and reflectivity. The method is based on two developments that facilitate robust multi-parameter inversion: (I) a wave-equation modelling relation parameterized in velocity and vector reflectivity and (II) a robust procedure

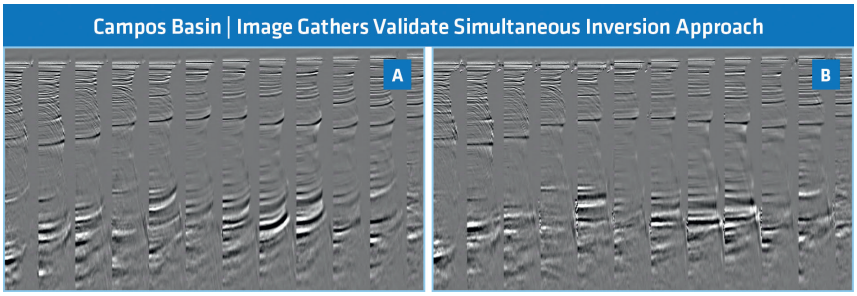


**Figure 5** Campos Basin field data example. Image gathers from the initial model (a) and the FWI model (b).

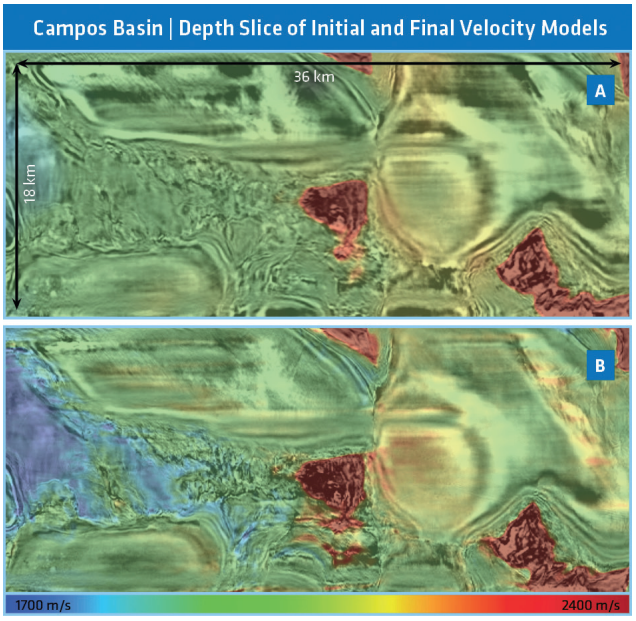


**Figure 6** Campos Basin field data example. (a) Depth slice of the initial velocity at 3.4 km plotted on the first iteration reflectivity. (b) Depth slice of the FWI model on the final inverted reflectivity.

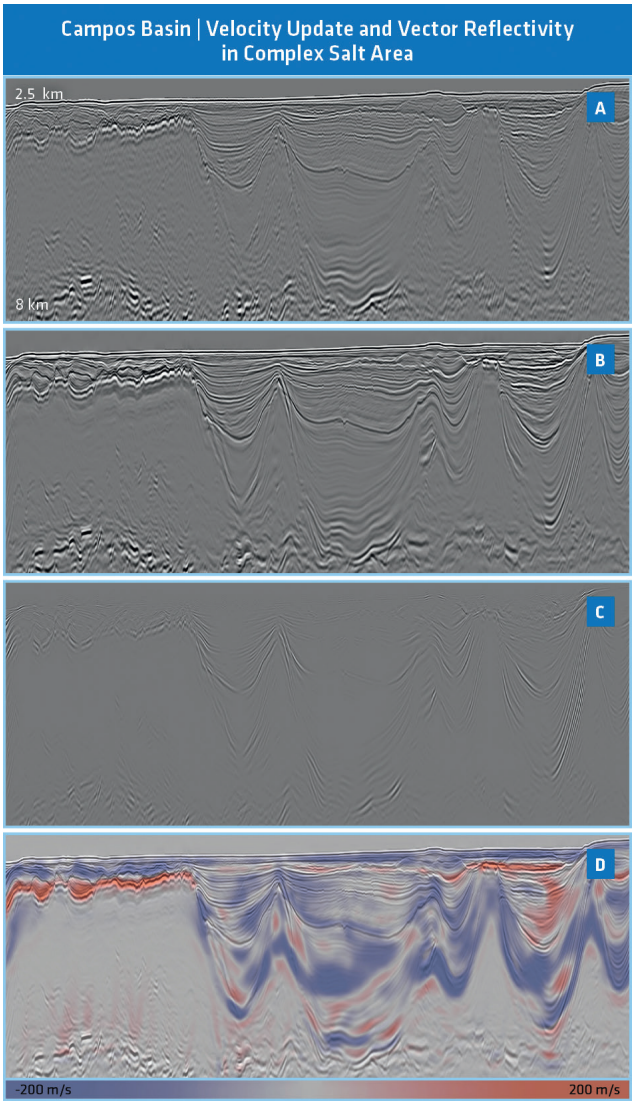


**Figure 7** Campos Basin field data example. Another inline section including updates inside the salt. (a) Vertical reflectivity from first iteration. (b) Final inverted vertical reflectivity. (c) Final inverted horizontal reflectivity along inline direction. (d) Velocity updates superimposed on final vertical reflectivity.

to separate the low- and high-wavenumber components of the inversion gradient. We successfully applied the simultaneous inversion to two field datasets. Results demonstrate that while the velocity model is iteratively updated, an accurate estimate of the earth's reflectivity is simultaneously generated. We demonstrated that FWI and LS-RTM can be performed jointly as a single inversion workflow using minimally processed data. Accordingly, the simultaneous inversion potentially reduces the turnaround time for model building and imaging projects.

The current implementation of simultaneous inversion is based on stacked vector reflectivity. A worthwhile future development is to extend the inversion to include elastic effects and angle gathers for better description of reservoirs.

## Acknowledgements

The authors wish to thank PGS for permission to publish the paper. We would also like to thank Tiago Alcantara, Tony Martin and Ramzi Djebbi for numerous discussions and valuable support.

## References

Berkhout, A.J. [2012]. Combining full wavefield migration and full waveform inversion, a glance into the future of seismic imaging. *Geophysics*, **77**(2), 43-50.

Chi, B., Gao, K. and Huang L. [2017]. Least-squares reverse time migration guided full-waveform inversion. 87th Annual International Meeting, SEG, Expanded Abstracts.

Mora, P. [1989]. Inversion=migration+tomography. *Geophysics*, **54**(12), 1575-1586.

Ramos-Martinez, J., Crawley, S., Zou, K., Valenciano, A.A., Qiu, L. and Chemingui, N. [2016]. A robust gradient for long wavelength FWI updates. 78th EAGE Conference & Exhibition, Extended Abstracts.

Tarantola, A. [1984]. Inversion of seismic reflection data in acoustic approximation. *Geophysics*, **49**(8), 1259-1266.

Verschuur, D.J., Staal, X.R. and Berkhout, A.J. [2016]. Joint migration inversion: Simultaneous determination of velocity fields and depth images using all orders of scattering. *The Leading Edge*, **35**, 1037-1046.

Whitmore, N.D. and Crawley, S. [2012]. Application of RTM inverse scattering imaging conditions. 82nd Annual International Meeting, SEG, Expanded Abstracts.

Whitmore, N.D., Ramos-Martinez, J., Yang, Y. and Valenciano, A.A. [2020]. Full wave field modeling with vector-reflectivity. 82nd EAGE Conference & Exhibition, Extended Abstracts.

Xu, S., Wang, D., Chen, F., Zhang, Y. and Lambaré, G. [2012]. Full waveform inversion for reflected seismic data. 74th Annual International Meeting, SEG, Expanded Abstracts.

Yang, Y., Ramos-Martinez, J., Whitmore, D., Valenciano, A.A. and Chemingui, N. [2020]. Full Waveform Inversion Using Wave Equation Reflectivity Modeling. 82nd EAGE Conference & Exhibition, Extended Abstracts.

Zhou, W., Brossier, R., Operto, S. and Virieux, J. [2015]. Full waveform inversion of diving and reflected waves for velocity model building with impedance inversion based on scale separation. *Geophysical Journal International,* **202**, 1535-1554.